Direct interaction with Hoxd proteins reverses Gli3-repressor function to promote digit formation downstream of Shh

Yuting Chen[1,‡], Vladimir Knezevic[1,*,‡], Valerie Ervin[1], Richard Hutson[1,†], Yvona Ward[2] and Susan Mackem[1,§]

[1]Laboratory of Pathology, Center for Cancer Research, NCI, NIH, Bethesda, MD 20892, USA
[2]Cell and Cancer Biology Branch, Center for Cancer Research, NCI, NIH, Bethesda, MD 20892, USA
*Present address: 20/20 Gene Systems Inc., Rockville, MD 20850, USA
†Present address: US Deptartment of Commerce, USPTO, Washington, DC 20231, USA
‡These authors contributed equally to this work
§Author for correspondence (e-mail: smack@helix.nih.gov)

Accepted 9 February 2004

Development 131, 2339-2347
Published by The Company of Biologists 2004
doi:10.1242/dev.01115

Summary

Sonic hedgehog (Shh) signaling regulates both digit number and identity, but how different distinct digit types (identities) are specified remains unclear. Shh regulates digit formation largely by preventing cleavage of the Gli3 transcription factor to a repressor form that shuts off expression of Shh target genes. The functionally redundant 5′Hoxd genes regulate digit pattern downstream of *Shh* and *Gli3*, through as yet unknown targets. Enforced expression of any of several 5′Hoxd genes causes polydactyly of different distinct digit types with posterior transformations in a *Gli3*(+) background, whereas, in *Gli3* null limbs, polydactylous digits are all similar, short and dysmorphic, even though endogenous 5′Hoxd genes are broadly misexpressed. We show that Hoxd12 interacts genetically and physically with Gli3, and can convert the Gli3 repressor into an activator of Shh target genes. Several 5′Hoxd genes, expressed differentially across the limb bud, interact physically with Gli3. We propose that a varying [Gli3]:[total Hoxd] ratio across the limb bud leads to differential activation of Gli3 target genes and contributes to the regulation of digit pattern. The resulting altered balance between 'effective' Gli3 activating and repressing functions may also serve to extend the Shh activity gradient spatially or temporally.

Key words: AP pattern, Digit formation, Limb development, Hoxd genes, Gli3, Sonic hedgehog. Mouse

Introduction

Digits arise as single chondrogenic condensations that later segment and grow differentially to acquire defining features, such as the number, size and shape of their phalanges (segments) (Dahn and Fallon, 2000) (see reviews by Mariani and Martin, 2003; Tickle, 2003). The pattern of different digits (I to V) that form from anterior (A; digit I, e.g. thumb) to posterior (P; digit V, e.g. little finger) is controlled by secreted Shh signals produced in the posterior limb bud mesoderm (reviewed by Ingham and McMahon, 2001; Mariani and Martin, 2003; Tickle, 2003). Shh regulates both digit number and identity in a dose-dependent manner; increasing levels of Shh expand digit-forming capacity and specify more posterior digit identities (Yang et al., 1997; Lewis et al., 2001). The zinc finger transcription factor Gli3 is the direct intracellular mediator of Shh (Altaba, 1999; Dai et al., 1999; Shin et al., 1999) (reviewed by Ingham and McMahon, 2001) and Shh signaling protects Gli3 from cleavage to a repressor form (Wang et al., 2000). Without *Shh*, Gli3 repressor predominates, Shh/Gli3 target genes are repressed (Altaba, 1999; Dai et al., 1999; Shin et al., 1999) and digit formation largely fails (Chiang et al., 2001; Kraus et al., 2001). Eliminating Gli3 renders *Shh* dispensable for digit formation, but normal digit identity is lost and polydactyly occurs (Litingtung et al., 2002; te Welscher et al., 2002). In addition to functioning antagonistically, Gli3 also represses *Shh* expression and, in $Gli3^{-/-}$ embryos, *Shh* is expressed ectopically in the anterior limb bud (Masuya et al., 1995). Although de-regulated *Shh* expression is a consequence of altered Gli3 function, it is not the principle cause for polydactyly, because $Gli3^{-/-}$;$Shh^{-/-}$ embryos are likewise polydactylous (Litingtung et al., 2002; te Welscher et al., 2002). In both $Gli3^{-/-}$ and $Gli3^{-/-}$;$Shh^{-/-}$ limbs, the digits are indistinguishable, dysmorphic and of indeterminate identity (Litingtung et al., 2002). Thus, other factors conferring normal digit identity, previously presumed to be mainly full-length Gli3 activator, are lacking or rendered nonfunctional in these mutants.

Several 5′Hoxd genes are expressed in posterior-distal domains in the early limb bud mesoderm, and play roles in regulating digit number and pattern downstream of Shh (Dolle et al., 1989; Nelson et al., 1996) (reviewed by Zakany and Duboule, 1999). Analysis of single- and compound-null mutants has revealed extensive functional overlap between different 5′Hox members, and indicates that they act in an additive, dose-dependent fashion (Fromental-Ramain et al., 1996; Zakany et al., 1997; Wellik and Capecchi, 2003) (reviewed by Zakany and Duboule, 1999). By contrast, forced expression of individual 5′Hoxd genes in the limb bud has more dramatic consequences; elevated *Hoxd11*, *Hoxd12* or *Hoxd13* levels each cause duplications and transformations of anterior digits to posterior identities (Morgan et al., 1992; Knezevic et al., 1997) (*Hoxd13*) (J. Innis, personal

communication). We previously showed that a *Hoxd12* transgene (*Tg-Hoxd12*), expressed throughout the limb bud, causes polydactyly and also ectopic anterior *Shh* expression (Knezevic et al., 1997). 5′Hoxd genes are downstream targets of Gli3, and their expression is broadly activated across the early limb bud in *Gli3*$^{-/-}$ embryos (Zuniga and Zeller, 1999). Yet in the *Gli3*$^{-/-}$ background, extended high-level Hoxd expression is not associated with the production of distinct digit identities, as is seen in a wild-type background. The assumption is that the presence of the full-length Gli3 activator is entirely responsible for such phenotypic differences. We present evidence that Gli3 and Hoxd12 interact genetically and physically, and that this interaction modulates Gli3 repressor function. By extension to other 5′Hoxd members, this finding provides a foundation for understanding how Hoxd proteins might function semi-quantitatively to regulate digit pattern and identity, and also has implications for how polydactyly may arise in certain human syndromes caused by mutations expected to produce a constitutive repressor form of Gli3.

Materials and methods

Analysis of mouse embryos

The generation, characteristics and genotyping of the *Tg-Hoxd12* line, and procedures for in situ hybridization and skeletal analysis of embryos, were all previously described (Knezevic et al., 1997). The *Gli3-Xt*^{J} line was obtained from Jackson Laboratories and genotyped as described (Litingtung et al., 2002; Buscher et al., 1998). Compound hemizygous *Tg-Hoxd12*;*Gli3*$^{+/-}$ embryos were generated in crosses between *Tg-Hoxd12* (inbred FVB/N) and *Xt*$^{+/-}$ (inbred C3H) mice. *Tg-Hoxd12;Gli3*$^{-/-}$ embryos were generated by crossing live born F1 *Tg-Hoxd12*;*Gli3*$^{+/-}$ mice (FVB/N-C3H mix) with *Xt*$^{+/-}$ mice (inbred C3H). Embryos from a large series of test crosses were first analyzed, to rule out effects due to genetic variation from the mixed F1 background on the phenotype of *Tg-Hoxd12* and of *Xt*$^{+/-}$. In primary crosses between wild-type FVB/N and *Xt*$^{+/-}$ (inbred C3H), the typical *Xt*-phenotype (single extra digit 1, all limbs) was consistently observed (23/45 total progeny). In primary crosses between wild-type C3H and *Tg-Hoxd12* (inbred FVB/N), all *Tg-Hoxd12* progeny displayed wild-type limb phenotypes, except for a single embryo with a triphalangeal digit 1 in one hind limb (1/52 Tg positives). The *Gli3*$^{-/-}$ limb phenotype, evaluated on mixed background, was also found to be indistinguishable from the inbred C3H background [15 *Gli3*$^{-/-}$ embryos from crosses of F1 *Xt*$^{+/-}$ (FVB/N-C3H mix)].

Expression plasmids and antibodies

Hoxd12/Gst fusion proteins contained chick Hoxd12 sequences C-terminal to Gst as follows: FL (full length), amino acids (aa) 9-266; ΔHD (homeodomain deleted), aa 9-151; and HD (homeodomain), aa 167-266. In all transfection experiments, the full-length protein constructs included aa 1-266 expressed in pSG5. Full-length Hoxa1 and Hoxb1 were also expressed from pSG5 (DiRocco et al., 1997). Hoxd12 mutated in the homeodomain (HD) to inactivate DNA binding capacity (mtHD) contained a two residue conservative substitution of WF to AA (aa 245-246) in helix 3 of the HD, generated using Quick Change mutagenesis (Stratagene). The resulting protein was expressed at the same level as wild type, but was non-functional in gel shift and transfection assays using Hoxd12-consensus element-driven reporters (data not shown). Hoxd13/Gst included chick sequences encoding aa 112-309, and this fusion protein was also used as an immunogen to generate the Hoxd13 antibody. Gst-fusion proteins were checked on gels to normalize the amounts of all fusions used in pull-down experiments (data not shown). Full-length and truncated (TR, aa 1-674) Gli3-expressing constructs in pcDNA3.1 (Shin et al., 1999) were used as described. Gli3 N-ZnF was generated by cleavage of Gli3 TR with *Bst*EII to produce a 426 aa run-off protein, in vitro, with all zinc fingers (ZnF) deleted. Hoxd12 polyclonal rabbit antibody was generated by immunization with the Hoxd12-ΔHD/Gst fusion protein and affinity-purified. The polyclonal affinity-purified Gli3 antibody used for some experiments was a gift from C. Chiang, or was generated using a Human GLI3/Gst (aa 1-497) fusion protein as an immunogen.

Protein interaction assays

Gst-fusion proteins loaded onto glutathione-sepharose beads were blocked with 2% BSA, and bound to ^{35}S-labeled in vitro translated proteins (Promega TNT) as indicated. For co-immunoprecipitation (co-IP) assays from transfected cells, cells were lysed [lysis buffer: 10 mM HEPES (pH 7.5), 1mM EDTA, 250 mM NaCl, 0.5% NP-40, protease inhibitors] on ice for 25 minutes with trituration, lysates were centrifuged at 5000 rpm for 5 minutes, and the supernatants bound to Protein G Agarose loaded with affinity-purified anti-Hoxd12 or affinity-purified anti-N peptide-Gli3 (Dai et al., 1999) antibodies. Bound proteins were detected on western blots with anti-Xpress-tag (Invitrogen), anti-Hoxd12, or anti-Hoxb1 (Covance) antibodies. For co-IP of endogenous embryonic proteins, limb bud tissues (see below) were dissected in PBS, pooled and lysed as above (~150 limb buds/ml), except that the lysis buffer salt concentration was increased to 420 mM NaCl. The Hoxd12 antibody used for co-IP was covalently cross-linked to beads (Pierce co-IP kit) and bound proteins were detected with affinity-purified anti-Gli3. Chick embryo protein lysates were made from separated anterior- or posterior-third early (stage 22) limb buds, or from later distal digital arch region, including condensations and interdigit mesenchyme (stage 27/28), that was used either intact or separated into anterior and posterior halves. In control experiments (not shown), Gli3 protein expression profiles in posterior limb bud halves from stage 21-24 were very similar to those in posterior thirds, and clearly displayed a very high ratio of full-length to repressor forms. All tissue lysates were prepared and analyzed on western blots as previously described (Wang et al., 2000; Litingtung et al., 2002), using polyclonal affinity-purified anti-Hoxd12, anti-Hoxd13 or anti-Gli3 antibodies.

Transfection assays

DF-1 cells (chick embryo fibroblast line, ATCC) were transfected (Qiagen Superfect) as indicated. For reporter assays, Ptc/luc (Shin et al., 1999) or 8×Gli/luc (Sasaki et al., 1997) values were normalized to pSV/RL (Promega dual reporter system). All reporter assays were performed in duplicate, and at least three independent experiments were performed to verify reproducibility.

Immunofluoresence co-localization

Co-transfected DF-1 cells were fixed in 4% paraformaldehyde, then co-incubated with Anti-Xpress (for tagged Gli3) and affinity-purified anti-Hoxd12 antibodies, followed by anti-rabbit-FITC and anti-mouse-Alexa Red secondary antibodies. Immunofluoresence was detected using a Zeiss Axiovert microscope (100×/1.4 oil immersion), and compared with control cultures of cells transfected singly with either the full-length Hoxd12 or the Gli3-TR expression vector; no differences in cellular localization were observed (data not shown). Confocal images were generated using a Zeiss LSM 510.

Results

Gli3-Hoxd12 genetic interaction

To investigate the possible basis for phenotypic similarities and differences resulting from Hoxd gain of function versus *Gli3* loss of function, we analyzed progeny from crosses between *Gli3*$^{+/-}$ and *Tg-Hoxd12* mice using a weakly expressing *Tg-Hoxd12* line (Knezevic et al., 1997) that, when hemizygous, has no abnormal phenotype alone (Fig. 1A). The *Gli3* null mutant

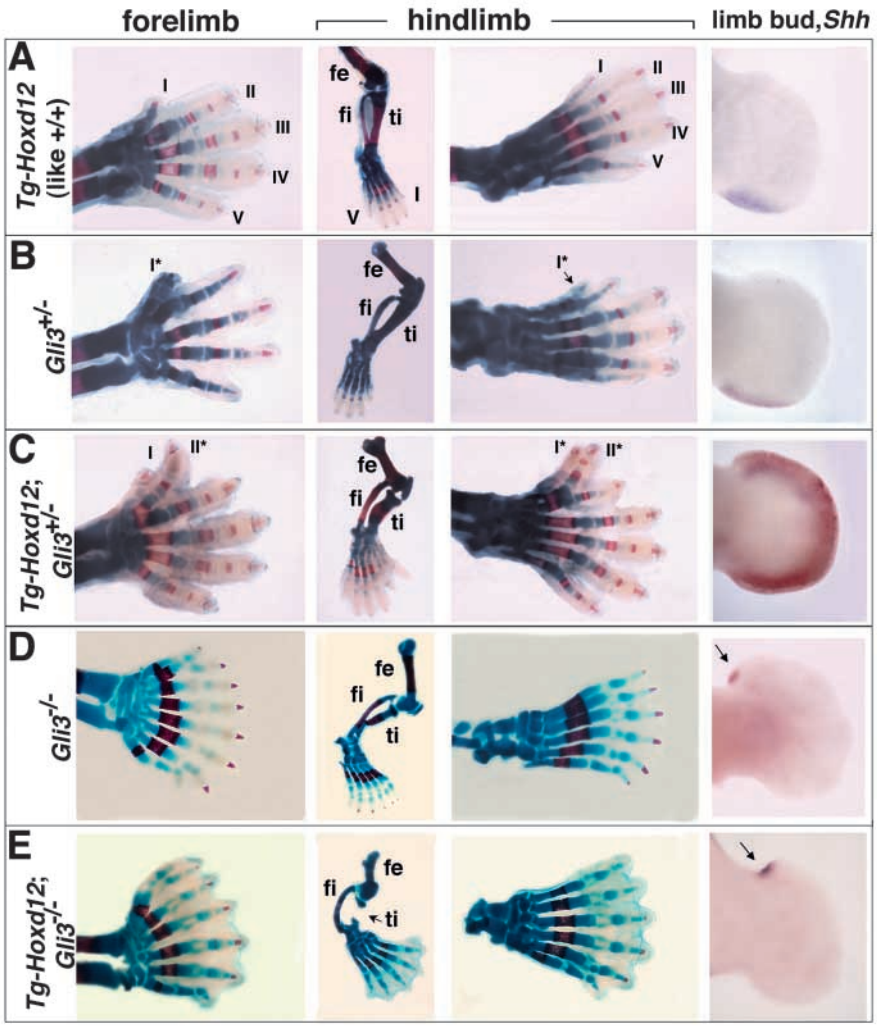

Fig. 1. *Gli3* and *Hoxd12* interact genetically during limb development. E17.5-18.5 limb skeletons (left and middle two columns), and E11.5-12.5 hindlimb bud *Shh* expression (right column) of (A) weak *Tg-Hoxd12* line (identical to wild type, +/+), (B) *Gli3*$^{+/-}$, (C) *Tg-Hoxd12*;*Gli3*$^{+/-}$, (D) *Gli3*$^{-/-}$ and (E) *Tg-Hoxd12*;*Gli3*$^{-/-}$ embryos. Hindlimb long bones (fe, femur; ti, tibia; fi, fibula) and digits (I-V) are marked for *Tg-Hoxd12*. Extra digits (*) with distinct identities are marked for *Gli3*$^{+/-}$ and *Tg-Hoxd12*;*Gli3*$^{+/-}$. Anterior is top, posterior bottom, for all panels except column 2 (anterior right, posterior left). *Gli3*$^{+/-}$ (B) have only an extra digit I (arrow), whereas *Tg-Hoxd12*;*Gli3*$^{+/-}$ (C) have more extensive polydactyly with posterior transformations and very distinct digit identities. By contrast, polydactyly in *Tg-Hoxd12*;*Gli3*$^{-/-}$ (E) is unchanged from *Gli3*$^{-/-}$ (D); both have 7-9 forelimb and 5-7 hindlimb digits that are all short and predominantly digit I-like (see also Fig. 2). Note that in some cases the posterior-most *Gli3*$^{-/-}$ digits show variable cartilage staining in an otherwise clear, amorphous region that is suggestive of a rudimentary third (middle) phalanx formation (e.g. D,E). In other instances (e.g. Fig. 2F), such rudiments are completely absent from all digits. Unlike digit phenotypes, long bone shortening worsens progressively, and is severest in *Tg-Hoxd12*;*Gli3*$^{-/-}$. Normal *Shh* expression (E11.5-12, right column) in *Tg-Hoxd12* (A) and *Gli3*$^{+/-}$ (B) is lost by E12.5, whereas some *Tg-Hoxd12*;*Gli3*$^{+/-}$ (C) have broad, deregulated *Shh* at ~E12. By contrast, *Tg-Hoxd12*;*Gli3*$^{-/-}$ (D) and *Gli3*$^{-/-}$ (E) both show only focal ectopic *Shh* (arrow) at E12.5.

used is haplo-insufficient (Hui and Joyner, 1993; Buscher et al., 1998) and *Gli3*$^{+/-}$ hemizygotes have a consistent, mild phenotype (single extra digit 1, all limbs; Fig. 1B). [The phenotypes of both these alleles were invariant in all backgrounds generated by the crosses used (described in Materials and methods).] By contrast, the compound hemizygous *Tg-Hoxd12*;*Gli3*$^{+/-}$ embryos had much more severe digit phenotypes than the single hemizygotes for either allele, including multiple digit duplications and posterior transformations (e.g. Fig. 1C, and Table 1). In the hindlimb, where the transgenic promoter used drives uniform expression of *Tg-Hoxd12* throughout the limb bud, 85% (22/26) of compound hemizygous *Tg-Hoxd12*;*Gli3*$^{+/-}$ embryos had severe phenotypes, whereas the remainder had a simple *Gli3*$^{+/-}$ phenotype (only extra digit 1). Compound hemizygous *Tg-Hoxd12*;*Gli3*$^{+/-}$ embryos also frequently displayed long bone shortening (especially tibia) in hindlimbs. In the forelimb, where the promoter driving *Tg-Hoxd12* expression is more postero-distally restricted and variable (Knezevic et al., 1997), 58% (15/26) of the compound hemizygotes had strong digit phenotypes.

Although *Shh* was normally expressed in both *Tg-Hoxd12* and *Gli3*$^{+/-}$ embryos (Fig. 1A,B), a strong synergistic deregulation of *Shh* was apparent in some of the compound hemizygous *Tg-Hoxd12*;*Gli3*$^{+/-}$ embryos, which showed broad *Shh* misexpression in one or both distal hindlimb buds (4/10 embryos, Fig. 1C). We cannot exclude a causative role for this *Shh* misexpression in production of the polydactyly, but several points argue against this. As is also the case in *Gli3*$^{-/-}$ embryos (Zuniga and Zeller, 1999), ectopic *Shh* expression occurred relatively late (only seen after E12) and thus may be a downstream consequence of altered *Gli3* function, rather than a cause of polydactyly. Furthermore, the frequency of *Shh* misexpression in compound hemizygous *Tg-Hoxd12*;*Gli3*$^{+/-}$ embryos was considerably lower than the incidence of subsequent severe digit phenotypes observed [for hindlimbs: 5/20 (25%) limb buds versus 38/52 (75%) skeletons]. In forelimbs, ectopic *Shh* expression was never detected even though severe digit skeletal phenotypes were sometimes seen (~50%, Table 1). This again suggests that although *Shh* deregulation was a consequence of Gli3-Hoxd interaction, it was not the primary cause for the skeletal abnormalities. Although not causative of digit phenotypes, the *Shh* misexpression occasionally seen in compound hemizygous *Tg-Hoxd12*;*Gli3* $^{+/-}$ embryos, but never in single hemizygotes, did suggest a genetic interaction (synergistic effect).

Table 1. Limb phenotypes of *Tg-Hoxd12;Gli3*$^{+/-}$ embryos

Embryo	Forelimb digits		Hindlimb digits		Tibia shortened
	Left	Right	Left	Right	
1	Xt-like	1,2*,2,3,4,5	2*,2*,2,3,4,5	1,2*,2,3,4,5	+
2	Xt-like	Xt-like	Xt-like	2*,1,2,3,4,5	+
3	1,2*,2,3,4,5	Xt-like	2*,1,2,3,4,5	2*,1,2,3,4,5	+
4	Xt-like	1,2*,2,3,4,5	Xt-like	2*,1,2,3,4,5	+
5	Xt-like	Xt-like	Xt-like	Xt-like	
6	Xt-like	Xt-like	2*,1,2,3,4,5	2*,1,2,3,4,5	+
7	Xt-like	Xt-like	Xt-like	Xt-like	
8	Xt-like	1,2*,2,3,4,5	2*,1,2,3,4,5	2*,2*,1,2,3,4,5	+
9	Xt-like	Xt-like	Xt-like	2*,1,2,3,4,5	
10	1,2*,2,3,4,5	Xt-like	2*,2*,1,2,3,4,5	1,2*,2,3,4,5	
11	Xt-like	1,2*,2,3,4,5	2*,2,3,4,5	2*,2*,2,3,4,5	
12	1,2*,2,3,4,5	Xt-like	2*,2,3,4,5	2*,1,2,3,4,5	+
13	Xt-like	1,1,1,2,3,4,5	2*,2*,2,3,4,5	2*,2*,2,3,4,5	+
14	Xt-like	Xt-like	2*,2*,2,3,4,5	2*,2*,2,3,4,5	+
15	Xt-like	1,1,1,2,3,4,5	Xt-like	2*,1,2,3,4,5	
16	Xt-like	1,1,2*,2,3,4,5	2*,1,2,3,4,5	1,2*,2,3,4,5	
17	Xt-like	Xt-like	2*,2*,2,3,4,5	2*,2*,2,3,4,5	
18	Xt-like	Xt-like	2*,2*,1,2,3,4,5	2*,2*,1,2,3,4,5	+
19	1,2*,2,3,4,5	Xt-like	2*,1,2,3,4,5	1,1,1,2,3,4,5	
20	1,2*,2,3,4,5	Xt-like	Xt-like	Xt-like	
21	Xt-like	1,2*,2,3,4,5	Xt-like	2*,2*,1,2,3,4,5	+
22	Xt-like	Xt-like	2*,2*,2,3,4,5	2*,2*,2,3,4,5	+
23	Xt-like	1,2*,2,3,4,5	2*,1,2,3,4,5	1,2*,1,2,3,4,5	+
24	Xt-like	1,2*,2,3,4,5	2*,2*,1,2,3,4,5	2*,1,1,2,3,4,5	+
25	Xt-like	Xt-like	1,1,1,2,3,4,5	Xt-like	
26	Xt-like	Xt-like	Xt-like	Xt-like	
Total Xt-like	11		4		NA
Total more severe	15		22		14

Mouse digits 2-4 are all triphalangeal, of a similar size, and consequently are difficult to distinguish. Therefore, additional polydactylous digits have arbitrarily been designated as digit 2 (when they are triphalangeal) to distinguish them from the biphalangeal digit 1 duplications typical of *Gli3*$^{+/-}$ embryos.

Xt-like, single extra anterior digit 1 indistinguishable from that observed with the hemizygous *Gli3*$^{+/-}$ *Xt*^{J} allele.

NA, not applicable (tibia of wild type and Gli3$^{+/-}$ are indistinguishable).

Gli3-Hoxd12 genetic interaction in digit formation requires functional Gli3

Unlike the compound hemizygous *Tg-Hoxd12*;*Gli3*$^{+/-}$, *Gli3*$^{-/-}$ (or likewise *Tg-Hoxd12*;*Gli3*$^{-/-}$, see below**)** embryos displayed polydactylous digits that were largely indistinguishable, short and highly dysmorphic (Fig. 1D,E; Fig. 2). At E18.5, all *Gli3*$^{-/-}$ digits had only a single ossification center, and an overall appearance suggesting two malformed phalangeal segments (rather than the normal three present in all digits posterior to digit I, see Fig. 2D-F). *Gdf5* expression, a marker for inter-phalangeal segmentation (Storm and Kingsley, 1996), was evaluated at E14.5 to confirm this impression. *Gdf5* staining revealed only one discrete, well-formed inter-phalangeal segment in *Gli3*$^{-/-}$ digits; a second more proximal zone of incomplete *Gdf5* staining suggested an abortive attempt at segmentation more proximally (Fig. 2A-C). Thus, *Gli3*$^{-/-}$ digits appear to have only two completely formed phalanges, although the high degree of dysmorphology makes this difficult to ascertain (see, for example, the variable, middle phalanx rudiment in some digits in Fig. 1D,E) (see also Litingtung et al., 2002). By contrast, the polydactylous digits in compound hemizygous *Tg-Hoxd12*;*Gli3*$^{+/-}$ embryos always had distinct identities and very well-defined phalanges at both E14.5 and E18.5 (compare Fig. 2B,E with C,F).

In contrast to the genetic interaction seen between *Tg-Hoxd12* and *Gli3*$^{+/-}$ in the compound hemizygotes, *Tg-Hoxd12*;*Gli3*$^{-/-}$ embryos had digital phenotypes that were indistinguishable from *Gli3*$^{-/-}$, both with respect to digit number and morphology (8/8; Fig. 1D,E), not withstanding more severely shortened long bones. This result is consistent with the fact that all *Gli3*$^{-/-}$ digits are similar and dysmorphic, despite the high level of endogenous Hoxd gene misexpression throughout *Gli3*$^{-/-}$ limb buds (Zuniga and Zeller, 1999; Litingtung et al., 2002; te Welscher et al., 2002). Likewise, ectopic *Shh* expression in *Tg-Hoxd12*;*Gli3*$^{-/-}$ embryos was very similar to that seen in *Gli3*$^{-/-}$ embryos and was restricted to a small anterior focus in the limb bud (12/12 embryos; Fig. 1D,E). The broad *Shh* misexpression apparent in a subset of compound hemizygous *Tg-Hoxd12*;*Gli3*$^{+/-}$ limb buds was not observed in *Tg-Hoxd12*;*Gli3*$^{-/-}$ embryos. Together, these results indicate that *Tg-Hoxd12* requires the presence of functional Gli3 protein (albeit at a reduced level) to exert effects on digit morphology and on *Shh* expression.

In vivo physical interaction between Gli3-Hoxd12

The strong genetic interaction and synergistic *Shh* activation seen only in compound hemizygous *Tg-Hoxd12*;*Gli3*$^{+/-}$ embryos but not in *Tg-Hoxd12*;*Gli3*$^{-/-}$ embryos, suggested a possible physical interaction between Hoxd12 and Gli3. When could Gli3-Hoxd interactions be physiologically relevant in the developing limb? At early patterning stages, Hoxd transcripts are expressed in nested posterior domains that overlap anteriorly with *Gli3*, which is expressed in the anterior three-quarters of the limb bud and is excluded from the posterior-

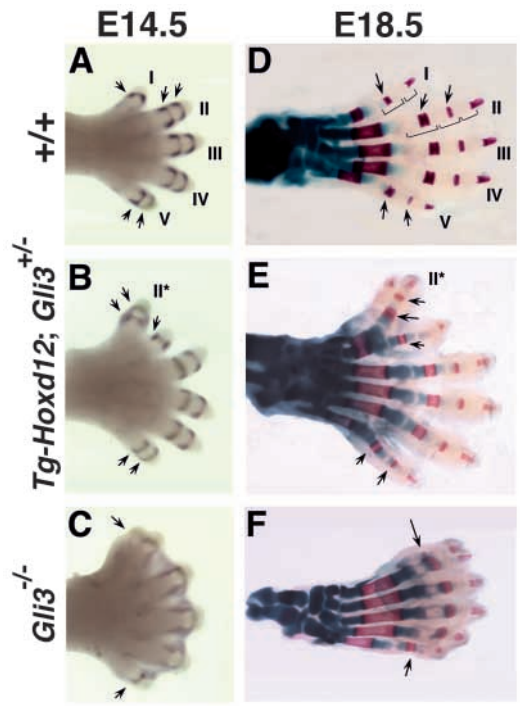

Fig. 2. Comparison of hindlimb digital morphologies in wild-type (+/+), *Tg-Hoxd12*;*Gli3*$^{+/-}$ and *Gli3*$^{-/-}$ embryos by *Gdf5* expression at E14.5 (A-C), and skeletal staining at E18.5 (D-F). Anterior is top, posterior bottom for all panels. At E14.5, bands of *Gdf5* expression in digits prefigure sites of future segmentation forming phalangeal joints (Storm and Kingsley, 1996). Both wild type (+/+; A) and *Tg-Hoxd12*;*Gli3*$^{+/-}$ (B) display one strong band of expression within digit I, and two bands in each of the more posterior digits (II-V). By contrast, *Gli3*$^{-/-}$ (C) has only one distinct band of expression and a second 'abortive' zone, which never forms a complete band across the digit (evaluated at multiple stages, data not shown). Note that, by E14.5, the proximal-most *Gdf5* expression band marking the phalangeal-metatarsal joint region in wild-type embryos has already declined. At E18.5, wild type (D) and *Tg-Hoxd12*;*Gli3*$^{+/-}$ (E) have distinguishable digits of varying size, with recognizable identities based on size, shape and number of phalanges. By contrast, *Gli3*$^{-/-}$ digits (F) are all short, similar in appearance, and have ill-defined phalanges with only a single ossification center. Arrows show ossification centers for digit I (single) compared with digit II-V (two centers), and brackets show phalangeal segments for digit I (2 segments) and digit II (3 segments) in wild type.

most mesoderm (Dolle et al., 1989; Nelson et al., 1996; Mo et al., 1997; Schweitzer et al., 2000) (see also Fig. 3A). Later, when digit condensations just begin to form, Hoxd transcripts are expressed in overlapping distal domains in the interdigit regions, and *Gli3* RNA is also strongly expressed, uniformly throughout all of the interdigit zones (see Fig. 3A) (see also Dolle et al., 1989; Nelson et al., 1996; Mo et al., 1997). This late expression overlap is potentially relevant to digit patterning because digit identity/morphology can still be regulated by interdigital mesenchymal signals at late stages (Dahn and Fallon, 2000). Full-length Gli3 is protected from cleavage to repressor by Hedgehog signaling (Wang et al., 2000) (reviewed by Ingham and McMahon, 2001); however, in late interdigit zones the extent of such signaling is unclear, as Shh expression in the posterior limb bud has declined and expression of Indian hedgehog (Ihh) produced in chondrogenic mesenchyme is just initiating. Therefore, interdigit Gli3 protein was evaluated to determine which form prevails at this stage. In early limb buds, the ratio of repressor to full-length Gli3 protein is dramatically regulated: high in the anterior and low in the posterior limb bud (see Fig. 3B) (see also Wang et al., 2000). The profile of Gli3 proteins present in interdigit mesenchyme (Fig. 3B) was both qualitatively and quantitatively very similar to Gli3 present in early anterior limb bud, even when the posterior interdigit region was analyzed separately. Thus, it is primarily the Gli3 repressor form that is likely to be active in interdigit zones at these later stages. As representatives of 5′Hoxd members, Hoxd12 and Hoxd13 protein levels were also checked, and expression was evident at both early (posterior limb bud) and late (interdigit) stages (Fig. 3B).

Interaction between endogenous Hoxd12 and Gli3 proteins was evaluated by co-immunoprecipitation from lysates of both early limb buds and late distal limb buds (Fig. 3C). At early stages, specific interaction of Hoxd12 was seen with both full-length and truncated Gli3 in limb bud lysates. In lysates from later distal interdigit zones, interaction was seen with truncated Gli3; this was as expected, as only trace levels of full-length Gli3 are present at this stage.

Domain requirements for Gli3-Hoxd protein interaction

To determine which protein domains in Gli3 and Hoxd12 were necessary for interaction, various in vitro translated Gli3 and Hoxd12/Gst-fusion protein domains (Fig. 4A) were tested in pull-down assays (Fig. 4B). The N-terminal, Zn-finger-containing region of Gli3 (Gli3 TR) and the C-terminal homeodomain region of Hoxd12 (HD) interacted (Fig. 4B). DNA-bridging did not explain this interaction, as a Gli3 N-terminal region lacking its zinc-finger DNA-binding domain still bound to a mutated Hoxd12 with inactivated DNA-binding (mtHD). Gli3 interacted preferentially with certain classes of homeodomains (Fig. 4C). Gli3 bound to Hoxd11/12/13, but only bound minimally to Hoxb1 or Hoxa1 when challenged in assays containing both 5′Hoxd (*AbdB* type) and 3′Hoxa/b (*Lab* type) proteins (Fig. 4C). Hoxd12 and Gli3 also co-immunoprecipitated specifically and selectively when co-expressed in transfected cells (Fig. 4D). Co-immunoprecipitation did not require Hoxd12 DNA-binding activity, and, when challenged, Hoxd12 was again selectively co-immunoprecipitated, even in the presence of co-transfected Hoxb1 protein (Fig. 4D). Gli3 and Hoxd12 also co-localized within the nucleus, but not the cytoplasm, of transfected cells (Fig. 4E). Hence the interaction with Hoxd12 did not act to sequester truncated Gli3-repressor protein in the cytoplasm, because the bulk of Gli3 protein was still nuclear and displayed a distribution comparable to Gli3 TR transfected alone (not shown).

Effect of Hoxd12 on Gli3 transcriptional repression

The Shh receptor *Ptc* is also a direct transcriptional target of Gli3, and is activated by Shh signals (Goodrich et al., 1996) (reviewed by Ingham and McMahon, 2001). A previously characterized Ptc/luciferase reporter (Shin et al., 1999), whose basal expression is induced threefold by full-length Gli3 and repressed up to 10-fold by the truncated repressor

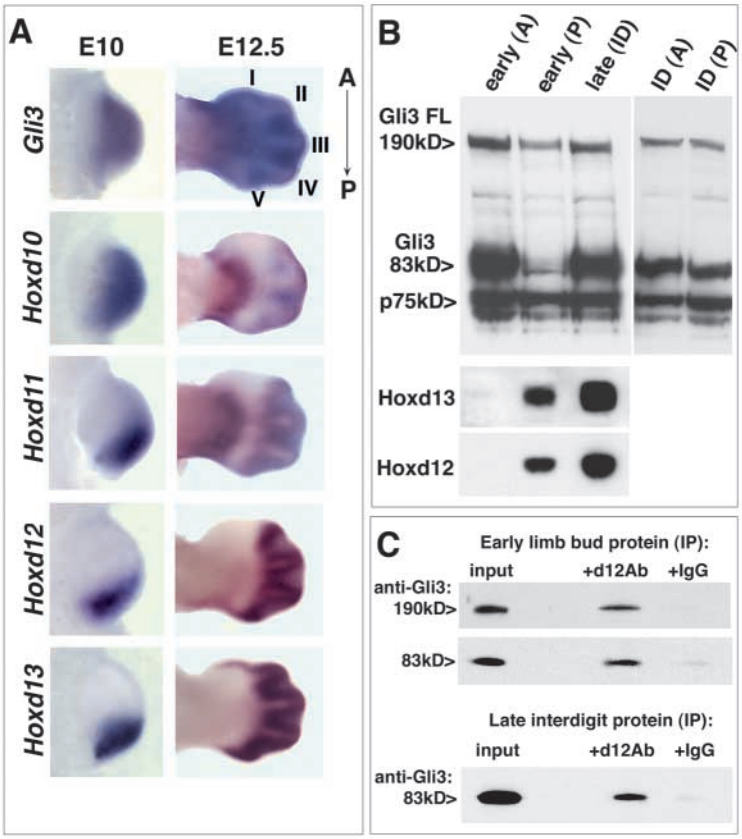

Fig. 3. Gli3-Hoxd expression overlap and interaction between endogenous Gli3-Hoxd12 proteins. (A) Expression of *Gli3*, and of *Hoxd10/11/12/13* RNA in nested posterior domains of E10 (left panel) and interdigits of E12 (right panel) forelimb buds (digit I-V, AP, indicated for Gli3). (B) Western blot comparing Gli3 protein in lysates from early chick (stage 22) anterior (A) or posterior (P) limb bud with late stage (27/28) distal digit arch region containing interdigit (ID) mesenchyme, either intact or separated into A and P parts. Lower panels show Hoxd12 and Hoxd13 proteins detected in the same lysates. Note these stages are comparable to mouse E10.5/E11 (early) and E12/E12.5 (late); chick and mouse RNA and protein expression profiles are generally similar (see Dolle et al., 1989; Nelson et al., 1996; Mo et al., 1997; Schweitzer et al., 2000; Wang et al., 2000; Litingtung et al., 2002). The ratio of the short-repressor form of Gli3 protein (83 kDa) relative to full length (190 kDa) in late interdigits is similar to the anterior early limb bud profile, consistent with lack of *Shh* expression at this stage. In posterior early limb buds, Shh activity results in a high ratio of full-length to repressor form of Gli3. p75kD is a Gli-related antigen of uncertain identity (Wang et al., 2000). (C) Co-immunoprecipitation (IP) of Gli3 and Hoxd12 from early (stage 22, upper panels) and late distal (stage 27/28, lower panel) chick limb bud lysates, using immobilized anti-Hoxd12 or control purified IgG for immunoprecipitation, and anti-Gli3 for detection of bound proteins. Endogenous Hoxd12 binds Gli3 from early limb bud, when both full-length (190kD) and repressor forms (83kD) of Gli3 are expressed, and from later interdigital zones, when mainly the repressor form of Gli3 protein is expressed.

form of Gli3 (Gli3 TR), was used to assess the effect of Hoxd12 binding to Gli3 on Gli3 target promoters in transfection assays. In our hands, activation of the reporter by full-length Gli3 was weak and variable, and the effect of co-transfected Hoxd12 was likewise variable and difficult to ascertain (Y.C. and S.M., unpublished). However, Gli3 TR reproducibly repressed basal expression, allowing evaluation of Hoxd12 effects on Gli3 transcriptional activity. Surprisingly, co-transfection of low levels of Hoxd12 with low levels of Gli3 TR converted the Gli3 repressor into an activator, with activity increasing according to the relative Gli3:Hoxd12 ratio (Fig. 5A). This stoichiometry determines whether activator (Gli3TR-Hoxd12 complex) or repressor (free Gli3 TR) function prevails. The DNA-binding activity of Hoxd12 was not required for this effect, as activation was comparable even when the DNA-binding mutant Hoxd12 was co-transfected with Gli3 TR (Fig. 5B). To further evaluate whether recruitment of Gli3 TR-Hoxd12 complexes to Gli3-regulated promoters requires only Gli3-binding sites or whether it might also depend on cryptic Hoxd12-binding elements, a basal promoter driven solely by multimerized Gli-consensus elements (Sasaki et al., 1997) was assayed. Whereas Gli3 TR alone repressed basal reporter expression, co-expressing low levels of the Hoxd12 DNA-binding mutant not only prevented repression, but upregulated expression above the basal level in the presence of Gli3 TR (Fig. 5C). Experiments in which the level of Gli3 TR was held constant while co-transfected Hoxd12 levels were increased likewise showed a decline in repression activity; however, it was not possible to vary Hoxd12 levels over a very broad range, owing to reporter activation by higher Hoxd12 levels that complicates interpretation of the results (data not shown).

Discussion

The results show a genetic interaction between a 5′Hoxd member and *Gli3* in regulating digit formation. Biochemical and transfection analyses further indicate that the 5′Hoxd class protein interacts physically with Gli3 via the homeodomain, and can convert the truncated Gli3 repressor form into an activator of its target promoters (Fig. 5D). This suggests a model in which Gli3-responsive target promoter activity would depend, at least in part, on the ratio of Gli3 to total Hoxd protein expression at a given site. This model is consistent with the known functional overlap and additive effects of 5′Hoxd genes (Zakany et al., 1997) (reviewed by Zakany and Duboule, 1999), as cumulative recruitment of Hoxd proteins to bound Gli3 repressor protein would modify the overall effect on Gli3 target promoters. Rather than a combinatorial Hox code, a quantitative Hox-activity gradient, determined by the total Hox protein relative to Gli3 protein at a particular site (Fig. 3A; and shown schematically in Fig. 6), would modify ‘net’ Gli3 function to regulate expression levels of Gli3 target promoters differentially, and thereby potentially activate downstream Shh pathway targets indirectly. The genetic evidence presented here suggests that Gli3-Hoxd interaction pertains mainly to the regulation of digit morphogenesis. This is not unexpected for an interaction with Gli3 shared among several posterior Hox proteins, given that some of the 5′Hoxd members normally only regulate digits physiologically (e.g. Hoxd13). In fact, the long

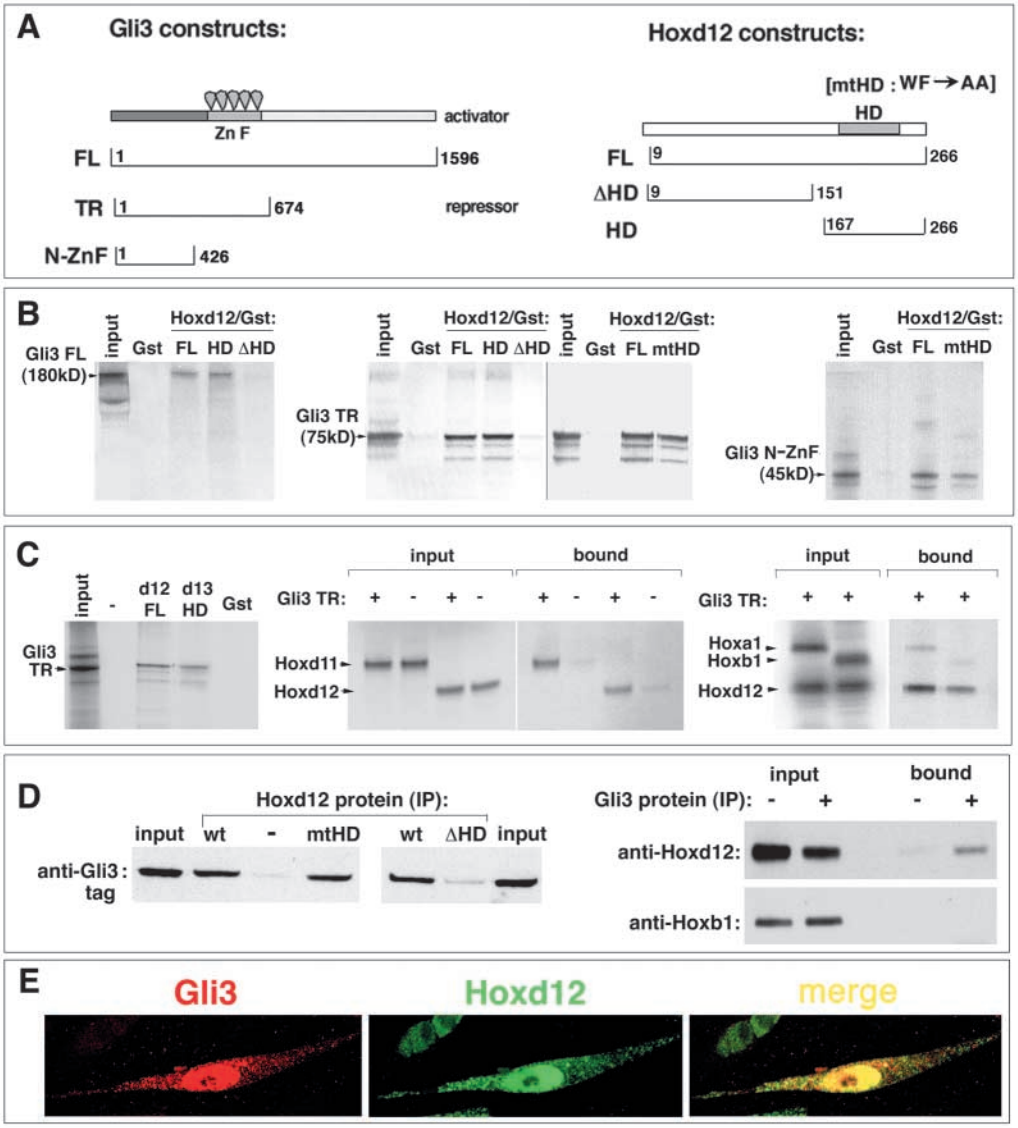

Fig. 4. Domains necessary for Gli3-Hoxd interaction. (A) Relevant Gli3 and Hoxd12 coding domains used in assays shown in B-D. All input lanes show 5-10% of the assay input (B-D). (B) The N-terminal Gli3 domain interacts with the C-terminal homeodomain (HD) of Hoxd12 in normalized Gst pull-down assays. The HD-region in Hoxd12/Gst is essential for interaction with in vitro translated (IVT) full-length (FL; B, left panel) or truncated (TR; B, middle panel) Gli3. Hoxd12 mutated in DNA-binding function (mtHD) and N-terminal Gli3 lacking zinc fingers (N-ZnF) still interact (B, middle, right panels). (C) 5′Hox proteins interact with Gli3 preferentially over 3′Hox proteins. Hoxd13(HD)/Gst fusion also binds Gli3 TR (C, left panel). IVT tagged-Gli3 TR (precipitated with Anti-Xpress) also binds full-length IVT Hoxd11 (C, middle panel). Hoxd12 binds preferentially in assays challenged with IVT full-length Hoxa1 or Hoxb1 (C, right panel). (D) Hoxd12 and Gli3 co-immunoprecipitate (IP) from co-transfected cells. Full-length wild-type (wt) or mutant (mtHD) Hoxd12 binds co-transfected Gli3 TR, whereas homeodomain-deleted Hoxd12 (ΔHD) does not (D, left panel). A representative input is shown; all inputs were similar and Hoxd12 recovery in IPs were equivalent (not shown). Hoxd12 binds Gli3 TR preferentially over co-transfected Hoxb1 (D, right panel). (E) Gli3 and Hoxd12 co-localize in transfected cell nuclei, as revealed in optical sections with FITC and Alexa Red antibodies. There are no differences in localization compared with the controls of cells transfected singly and expressing either Gli3 TR or Hoxd12 (full length) alone (data not shown).

bone shortening observed may represent a distinct dominant-negative effect independent of Gli3 (see Goff and Tabin, 1997). Gli3-Hox interactions may represent a recent evolutionary acquisition that, together with the distal recruitment of 5′Hox genes, enables the development of the distal autopod with its multiple digits. As the distal autopod is probably a neomorphic structure of tetrapod vertebrates (e.g. Sordino et al., 1995), it is not surprising that an interaction between the homologous *Drosophila* Ci and AbdB proteins has not been described.

In early limb buds, predominantly anterior *Gli3* expression and posterior Hoxd expression clearly overlap at their borders (Fig. 3A). Some Gli3 repressor form is present in the mid-limb bud region (Wang et al., 2000) where the Gli3-Hoxd overlap occurs. The co-expression of Hoxd members along with the Gli3 repressor in this border-zone could serve to modify (extend anteriorly) the effective Shh activity gradient across the early limb bud anteroposterior (AP) axis, and could thereby contribute to the specification of digit number and/or pattern (Fig. 6). The observed polydactyly ensuing from the enforced expression of any one of the several 5′Hoxd members may then be the result of enhanced binding to Gli3, and mitigation of repression in the early anterior limb bud. Enforced expression of *Hoxd12* does not result in any apparent change in the expression pattern or levels of Gli3 transcripts (V.K. and S.M., unpublished). By contrast, Gli3 does normally repress, and so restrict Hoxd expression to the posterior limb bud at early stages (Zuniga and Zeller, 1999); this regulatory relationship will serve to limit the extent of overlap and interaction between the Gli3 repressor and Hoxd proteins in the wild-type early limb bud. However, the same simple regulatory hierarchy is clearly not operational at later stages in the normal limb bud, because the interdigital expression of the endogenous Gli3 repressor and Hoxd members overlaps quite extensively in the wild-type embryo (e.g. Fig. 3A,B).

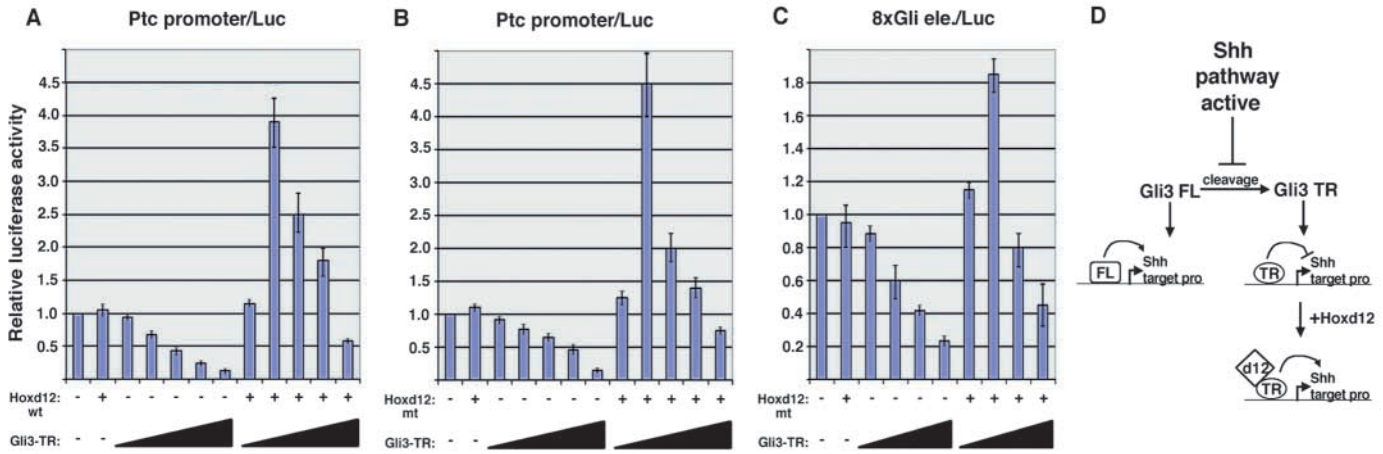

Fig. 5. Hoxd12 converts Gli3 repressor into an activator. (A,B) A 4 kb Ptc promoter/luciferase reporter (0.5 μg,) was co-transfected with varying amounts of Gli3 TR repressor (5-80 ng), with or without 25 ng of full-length Hoxd12 wild type (wt; A) or homeodomain mutant (mt; B). (C) Delta-crystallin basal promoter with eight Gli consensus elements (8×Gli)/luciferase (1.5 μg) co-transfected with full-length mt Hoxd12 (25 ng) and varying amounts of Gli3 TR (2.5-20 ng). (D) The transfection results are most consistent with a model in which Gli3 recruits Hoxd12 to Gli3-target DNA-binding sites, and the bound Hoxd12 converts Gli3 TR into an activator of the Gli3-target promoters in a stoichiometric fashion that is independent of Hoxd12 DNA binding.

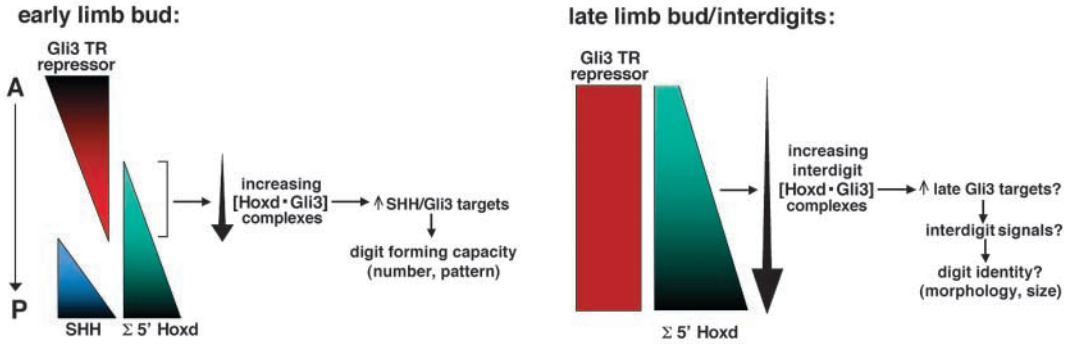

Fig. 6. Hoxd and Gli3 limb expression suggest a quantitative model for modification of Gli3 repressor function by total Hoxd10/11/12/13 protein expression. Schematics show the expected gradient of Gli3:[total Hoxd] complexes across the limb bud AP axis at early (left) and late interdigit (right) stages, and possible Gli3-regulated processes that may be affected by the varying Gli3-Hoxd stoichiometry across the limb bud. This model is compatible with the known functional overlap, and the incremental additive effects of posterior Hox genes in regulating digit morphogenesis (e.g. Zakany et al., 1997).

Indeed, some features of digit identity/morphology are determined late. Manipulation of interdigit mesenchyme in chick has revealed that adjacent interdigit regions instruct digit anlage to develop different distinct identitites (Dahn and Fallon, 2000), as judged by the number of phalangeal segments formed. The responsible interdigit signaling factors remain to be elucidated, but any regulation by Shh must be very indirect, as *Shh* expression has subsided by this stage. Expression of several Hoxd genes persists late in the interdigits, along with the Gli3 repressor (Fig. 3A), and this interaction could play a role in positively regulating the expression of late-secreted interdigit signals that determine different digit identities (Fig. 6). In this manner, Gli3-Hoxd interactions could function either to indirectly sustain the Shh pathway at these later stages, or, alternatively, to regulate novel (non-Shh mediated) targets. A major focus for future work will be determining the relative contributions and potential roles of early and later Gli3-Hoxd interactions in regulating digit formation and morphogenesis. Considering the redundancy of the posterior Hox genes, such approaches will entail a mutational analysis of Gli3 residues mediating the interaction.

Gli3-Hoxd interactions may also have implications for digit abnormalities in certain human syndromes arising from mutations in *GLI3*. Pallister-Hall Syndrome (PHS) and Post-Axial Polydactyly (PAP) behave semi-dominantly (reviewed by Biesecker, 1997), and arise from mutations expected to produce a truncated, constitutive-repressor form of GLI3 (Altaba, 1999; Dai et al., 1999; Shin et al., 1999). Recent mouse and chick models for PHS (Bose et al., 2002; Meyer and Roelink, 2003) confirm the constitutive-repressor function of this mutated *Gli3* gene in many developmental processes, where the homozygous PHS allele causes phenotypes resembling $Shh^{-/-}$ (Shh/Gli3 targets are repressed). However, surprisingly, the PHS allele does not block the Shh pathway in the limb, but instead results in polydactyly with non-identical digits (Bose et al., 2002). Whether or not such *Gli3* mutations behave as dominant repressors during limb development may depend on their interactions with Hoxd genes. In the limb, where Hoxd genes are uniquely expressed, the function of an otherwise dominant-repressor Gli3 mutant could be modified by an enhanced Hoxd-interaction affinity.

We thank L. Biesecker, C. Chiang, D. Duboule, C. C. Hui, S. Ishii, D. Kingsley, A. McMahon, H. Sasaki, E. Toftgard and V. Zappavigna for reagents; C. Chiang for discussions; J. Innis for sharing unpublished results; and C. Deng, J. Fallon, D. Levens, L. Liotta and Y. Yang for comments on the manuscript.

References

Altaba, A. R. I. (1999). Gli proteins encode context-dependent positive and negative functions: implications for development and disease. *Development* **126**, 3205-3216.

Biesecker, L. G. (1997). Strike three for GLI3. *Nat. Genet.* **17**, 259-260.

Bose, J., Grotewold, L. and Ruther, U. (2002). Pallister-Hall syndrome phenotype in mice mutant for Gli3. *Hum. Mol. Genet.* **11**, 1129-1135.

Buscher, D., Grotewold, L. and Ruther, U. (1998). The Xt(J) allele generates a Gli3 fusion transcript. *Mamm. Genome* **9**, 676-678.

Chiang, C., Litingtung, Y., Harris, M. P., Simandl, B. K., Li, Y., Beachy, P. A. and Fallon, J. F. (2001). Manifestation of the limb prepattern: limb development in the absence of sonic hedgehog function. *Dev. Biol.* **236**, 421-435.

Dahn, R. D. and Fallon, J. F. (2000). Interdigital regulation of digit identity and homeotic transformation by modulated BMP signaling. *Science* **289**, 438-441.

Dai, P., Akimaru, H., Tanaka, Y., Maekawa, T., Nakafuku, M. and Ishii, S. (1999). Sonic hedgehog-induced activation of the Gli1 promoter is mediated by GLI3. *J. Biol. Chem.* **274**, 8143-8152.

DiRocco, G., Mavilio, F. and Zappavigna, V. (1997). Functional dissection of a transcriptionally active, target-specific Hox-Pbx complex. *EMBO J.* **16**, 3644-3654.

Dolle, P., Izpisua-Belmonte, J. C., Falkenstein, H., Renucci, A. and Duboule, D. (1989). Coordinate expression of the murine Hox-5 complex homoeobox-containing genes during limb pattern-formation. *Nature* **342**, 767-772.

Fromental-Ramain, C., Warot, X., Messadecq, N., LeMeur, M., Dolle, P. and Chambon, P. (1996). Hoxa-13 and Hoxd-13 play a crucial role in the patterning of the limb autopod. *Development* **122**, 2997-3011.

Goff, D. J. and Tabin, C. J. (1997). Analysis of Hoxd-13 and Hoxd-11 misexpression in chick limb buds reveals that Hox genes affect both bone condensation and growth. *Development* **124**, 627-636.

Goodrich, L. V., Johnson, R. L., Milenkovic, L., McMahon, J. A. and Scott, M. P. (1996). Conservation of the hedgehog/patched signaling pathway from flies to mice: induction of a mouse patched gene by Hedgehog. *Genes Dev.* **10**, 301-312.

Hui, C. C. and Joyner, A. L. (1993). A mouse model of Greig cephalapolysyndactyly syndrome: the extra-toes' mutation contains an intragenic deletion of the Gli3 gene. *Nat. Genet.* **3**, 241-246.

Ingham, P. W. and McMahon, A. P. (2001). Hedgehog signaling in animal development: paradigms and principles. *Genes Dev.* **15**, 3059-3087.

Knezevic, V., De Santo, R., Schughart, K., Huffstadt, U., Chiang, C., Mahon, K. A. and Mackem, S. (1997). Hoxd-12 differentially affects preaxial and postaxial chondrogenic branches in the limb and regulates Sonic hedgehog in a positive feedback loop. *Development* **124**, 4523-4536.

Kraus, P., Fraidenraich, D. and Loomis, C. A. (2001). Some distal limb structures develop in mice lacking Sonic hedgehog signaling. *Mech. Dev.* **100**, 45-58.

Lewis, P. M., Dunn, M. P., McMahon, J. A., Logan, M., Martin, J. F., St-Jacques, B. and McMahon, A. P. (2001). Cholesterol modification of sonic hedgehog is required for long-range signaling activity and effective modulation of signaling by Ptc1. *Cell* **105**, 599-612.

Litingtung, Y., Dahn, R. D., Li, Y. N., Fallon, J. F. and Chiang, C. (2002). Shh and Gli3 are dispensable for limb skeleton formation but regulate digit number and identity. *Nature* **418**, 979-983.

Mariani, F. V. and Martin, G. R. (2003). Deciphering skeletal patterning: clues from the limb. *Nature* **423**, 319-325.

Masuya, H., Sagai, T., Wakana, S., Moriwaki, K. and Shiroishi, T. A. (1995). Duplicated zone of polarizing activity in polydactylous mouse mutants. *Genes Dev.* **9**, 1645-1653.

Meyer, N. P. and Roelink, H. (2003). The amino-terminal region of Gli3 antagonizes the Shh response and acts in dorsoventral fate specification in the developing spinal cord. *Dev. Biol.* **257**, 343-355.

Mo, R., Freer, A. M., Zinyk, D. L., Crackower, M. A., Michaud, J., Heng, H. H. Q., Chik, K. W., Shi, X. M., Tsui, L. C., Cheng, S. H., Joyner, A. L. and Hui, C. C. (1997). Specific and redundant functions of Gli2 and Gli3 zinc finger genes in skeletal patterning and development. *Development* **124**, 113-123.

Morgan, B. A., Izpisua-Belmonte, J. C., Duboule, D. and Tabin, C. J. (1992). Targeted misexpression of Hox-4.6 in the avian limb bud causes apparent homeotic transformations. *Nature* **358**, 236-239.

Nelson, C. E., Morgan, B. A., Burke, A. C., Laufer, E., DiMambro, E., Murtaugh, L. C., Gonzales, E., Tessarollo, L., Parada, L. F. and Tabin, C. (1996). Analysis of Hox gene expression in the chick limb bud. *Development* **122**, 1449-1466.

Sasaki, H., Hui, C. C., Nakafuku, M. and Kondoh, H. (1997). A binding site for Gli proteins is essential for HNF-3 beta floor plate enhancer activity in transgenics and can respond to Shh in vitro. *Development* **124**, 1313-1322.

Schweitzer, R., Vogan, K. J. and Tabin, C. J. (2000). Similar expression and regulation of Gli2 and Gli3 in the chick limb bud. *Mech. Dev.* **98**, 171-174.

Shin, S. H., Kogerman, P., Lindstrom, E., Toftgard, R. and Biesecker, L. G. (1999). GLI3 mutations in human disorders mimic Drosophila Cubitus interruptus protein functions and localization. *Proc. Natl. Acad. Sci. USA* **96**, 2880-2884.

Sordino, P., Vanderhoeven, F. and Duboule, D. (1995). Hox gene-expression in teleost fins and the origin of vertebrate digits. *Nature* **375**, 678-681.

Storm, E. E. and Kingsley, D. M. (1996). Joint patterning defects caused by single and double mutations in members of the bone morphogenetic protein (BMP) family. *Development* **122**, 3969-3979.

te Welscher, P. T., Zuniga, A., Kuijper, S., Drenth, T., Goedemans, H. J., Meijlink, F. and Zeller, R. (2002). Progression of vertebrate limb development through SHH-mediated counteraction of GLI3. *Science* **298**, 827-830.

Tickle, C. (2003). Patterning systems – from one end of the limb to the other. *Dev. Cell* **4**, 449-458.

Wang, B. L., Fallon, J. F. and Beachy, P. A. (2000). Hedgehog-regulated processing of Gli3 produces an anterior/posterior repressor gradient in the developing vertebrate limb. *Cell* **100**, 423-434.

Wellik, D. M. and Capecchi, M. R. (2003). Hox10 and Hox11 genes are required to globally pattern the mammalian skeleton. *Science* **301**, 363-367.

Yang, Y., Drossopoulou, G., Chuang, P. T., Duprez, D., Marti, E., Bumcrot, D., Vargesson, N., Clarke, J., Niswander, L., McMahon, A. and Tickle, C. (1997). Relationship between dose, distance and time in Sonic Hedgehog-mediated regulation of anteroposterior polarity in the chick limb. *Development* **124**, 4393-4404.

Zakany, J. and Duboule, D. (1999). Hox genes in digit development and evolution. *Cell Tissue Res.* **296**, 19-25.

Zakany, J., Fromental-Ramain, C., Warot, X. and Duboule, D. (1997). Regulation of number and size of digits by posterior Hox genes: a dose-dependent mechanism with potential evolutionary implications. *Proc. Natl. Acad. Sci. USA* **94**, 13695-13700.

Zuniga, A. and Zeller, R. (1999). Gli3 (Xt) and formin (Id) participate in the positioning of the polarising region and control of posterior limb-bud identity. *Development* **126**, 13-21.